

Vestibular evidence for the evolution of aquatic behaviour in early cetaceans

F. Spoor*, S. Bajpai†, S. T. Hussain‡, K. Kumar§ & J. G. M. Thewissen||

* Department of Anatomy & Developmental Biology, University College London, Rockefeller Building, University Street, London WC1E 6JJ, UK

† Department of Earth Sciences, Indian Institute of Technology, Roorkee 247 667, India

‡ Department of Anatomy, College of Medicine, Howard University, Washington DC 20059, USA

§ Wadia Institute of Himalayan Geology, Dehradun 248 001, India

|| Department of Anatomy, Northeastern Ohio Universities College of Medicine, Rootstown, Ohio 44272, USA

Early cetaceans evolved from terrestrial quadrupeds to obligate swimmers, a change that is traditionally studied by functional analysis of the postcranial skeleton¹. Here we assess the evolution of cetacean locomotor behaviour from an independent perspective by looking at the semicircular canal system, one of the main sense organs involved in neural control of locomotion². Extant cetaceans are found to be unique in that their canal arc size, corrected for body mass, is approximately three times smaller than in other mammals. This reduces the sensitivity of the canal system, most plausibly to match the fast body rotations that characterize cetacean behaviour. Eocene fossils show that the new sensory regime, incompatible with terrestrial competence, developed quickly and early in cetacean evolution, as soon as the taxa are associated with marine environments. Dedicated agile swimming of cetaceans thus appeared to have originated as a rapid and fundamental shift in locomotion rather than as the gradual transition suggested by postcranial evidence. We hypothesize that the unparalleled modification of the semicircular canal system represented a key 'point of no return' event in early

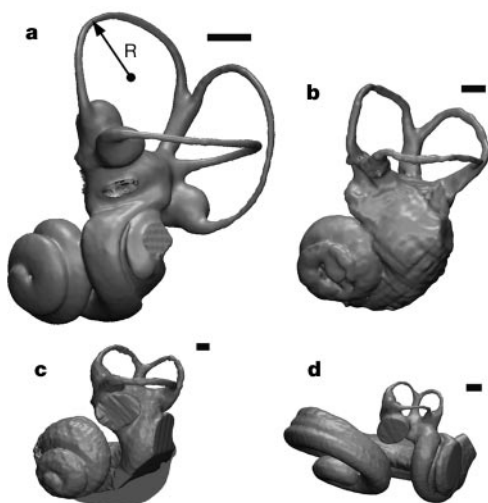


Figure 1 Lateral view of left bony labyrinths. **a**, *Galago moholi*, a particularly agile non-cetacean mammal; **b**, *Ichthyolestes pinfoldi*; **c**, *Indocetus ramani* (inferior part of basal turn partially reconstructed); **d**, extant *Tursiops truncatus*. The size of the labyrinths is corrected for body mass according to the mammalian regression given in Fig. 2a. Scale bars are 1 mm. The radius of curvature (R) of the anterior semicircular canal, expressing its arc size, is indicated for *Galago*. The apex of the cochlea faces inferiorly rather than laterally in *Tursiops*.

cetacean evolution, leading to full independence from life on land.

Early cetacean evolution, marked by the emergence of obligate aquatic behaviour, represents one of the major morphological shifts in the radiation of mammals. Modifications to the postcranial skeleton during this process are increasingly well-documented^{3–9}. Pakicetids, early Eocene basal cetaceans, were terrestrial quadrupeds with a long neck and cursorial limb morphology⁹. By the late middle Eocene, obligate aquatic dorudontids approached modern cetaceans in body form, having a tail fluke, a strongly shortened neck, and near-absent hindlimbs¹⁰. Taxa which represent bridging nodes on the cladogram show intermediate morphologies, which have been inferred to correspond with otter-like swimming combined with varying degrees of terrestrial capability^{4–8,11}. Our knowledge of the behavioural changes that crucially must have driven the postcranial adaptations is based on functional analysis of the affected morphology itself. This approach is marred by the difficulty of recognizing whether plesiomorphic morphologies were either simply retained from the ancestor, or actively selected for in their original or a newly acquired functional role. We therefore sought to assess early cetacean locomotor behaviour using an alternative and independent source, by examining the semicircular canal system, part of the vestibular apparatus (organ of balance) housed in the

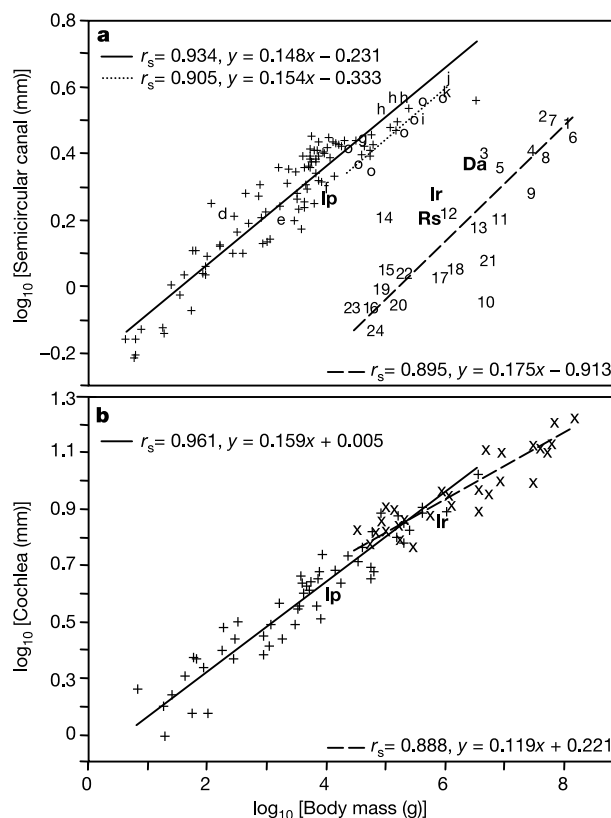


Figure 2 Relationship of semicircular canal and cochlea sizes to body mass.

a, **b**, Bivariate double logarithmic plots between body mass and the mean radius of curvature of the three semicircular canals (**a**), and the size of the cochlea (**b**). Codes for cetacean species are given in Table 1. Data points are labelled as follows: x, extant cetaceans; o, artiodactyls; crosses, other mammal species; d, *Galago moholi* (shown in Fig. 1a); e, *Ornithorhynchus anatinus*; f, *Lutra lutra*; g, *Hydrochaeris hydrochaeris*; h, Phocidae; i, *Dugong dugon*; j, *Hippopotamus amphibius*; k, *Odobenus rosmarus*; e–k, amphibious or aquatic non-cetaceans. The Spearman rank correlation coefficients (r_s) and reduced major axis regressions are given for the extant cetaceans (dashed line), the non-cetacean mammals (solid line) and the artiodactyls (dotted line); **a**,

letters to nature

inner ear. It records angular motion of the head and contributes, through reflex mechanisms, to the sensory control of locomotion, including the stabilization of the head and eyes². The arc size of semicircular canals is a determinant of their sensitivity^{12,13} and has been found to correlate with the degree of locomotor agility^{14,15}.

Cetacean semicircular canals have been noted as small in size^{16–23}, but this phenomenon has been studied neither quantitatively nor systematically. We therefore compared the canal sizes of 24 extant cetaceans and 106 other mammalian species, representing all major

Table 1 The cetacean species and other mammalian orders analysed

	Semicircular canal	Cochlea	Code
Monotremata	1	–	
Didelphimorphia	3	3	
Notoryctemorphia	1	1	
Dasyuromorphia	3	3	
Peramelemorphia	1	1	
Insectivora	2	2	
Chiroptera	7	2	
Scandentia	1	–	
Primates	43	11	
Xenarthra	3	2	
Lagomorpha	2	2	
Rodentia	12	6	
Carnivora (Fissipedia)	12	10	
Pinnipedia	4	3	
Proboscidea	1	1	
Sirenia	1	1	
Perissodactyla	1	1	
Artiodactyla	8	5	
Balaenidae			
<i>Balaena mysticetus</i>	1	–	1
<i>Eubalaena glacialis</i>	2	2	2
Neobalaenidae			
<i>Caperea marginata</i>	1	1	3
Eschrichtiidae			
<i>Eschrichtius robustus</i>	1	1	4
Balaenopteridae			
<i>Balaenoptera acutorostrata</i>	1	1	5
<i>Balaenoptera borealis</i>	–	1	–
<i>Balaenoptera musculus</i>	1	1	6
<i>Balaenoptera physalis</i>	1	1	7
<i>Megaptera novaeangliae</i>	2	2	8
Physeteridae			
<i>Physeter catodon</i>	1	1	9
Kogiidae			
<i>Kogia</i> sp.	1	1	10
Ziphiidae			
<i>Berardius bairdi</i>	1	1	11
<i>Mesoplodon densirostris</i>	1	1	12
<i>Ziphius cavirostris</i>	1	1	13
Platanistidae			
<i>Platanista gangetica</i>	1	1	14
Iniidae			
<i>Inia geoffrensis</i>	1	1	15
Pontoporiidae			
<i>Pontoporia blainvillei</i>	1	1	16
Monodontidae			
<i>Delphinapterus leucas</i>	1	1	17
<i>Monodon monoceros</i>	1	1	18
Delphinidae			
<i>Delphinus</i> sp.	1	2	19
<i>Feresa attenuata</i>	–	1	–
<i>Globicephala</i> sp.	–	1	–
<i>Grampus griseus</i>	–	1	–
<i>Lagenorhynchus obliquidens</i>	1	1	20
<i>Orcinus orca</i>	1	1	21
<i>Stenalla</i> sp.	–	1	–
<i>Tursiops truncatus</i>	3	3	22
Phocoenidae			
<i>Neophocaena phocaenoides</i>	1	1	23
<i>Phocoena phocoena</i>	1	1	24
Pakicetidae			
<i>Ichthyolestes pinfoldi</i> HGSP96434	1	1	lp
Remingtonocetidae			
<i>Remingtonocetus</i> sp. RUSB2529	1	–	Rs
Protocetidae			
<i>Indocetus ramani</i> LUV11034	1	1	lr
Dorudontidae			
<i>Dorudon atrox</i> BM(NH)-M9266	1	–	Da

The number of specimens are given for the cetaceans, and the number of species for the other mammalian orders, listed separately for the semicircular canal and cochlea measurements. The codes used in Fig. 1 are indicated for the cetaceans. A full list of the measurements is available as Supplementary Information.

orders (Table 1; Fig. 1a, d; Supplementary Information). In cetaceans the canal arc size scales with body mass with similar, strong negative allometry, as it does in other mammals (Fig. 2a). However, the canal arcs are, on average, three times smaller than those of other mammals of the same body mass, without overlap between the respective ranges of interspecific variation. Hence, the semicircular canals of the blue whale (*Balaenoptera musculus*) are just smaller than the average human size, and those of the bottle-nosed dolphin (*Tursiops truncatus*) are considerably smaller than in the brown rat. We also measured the semicircular canal size of four Eocene cetaceans. They represent respective nodes on the cetacean phylogenetic tree, and are: *Ichthyolestes*, a pakicetid from Pakistan; *Remingtonocetus*, a remingtonocetid from India; *Indocetus*, a protocetid from India; and *Dorudon*, a dorudontid from Egypt (Figs 1b, c and 3). The oldest of these, *Ichthyolestes*, shows a canal size similar to that of the closest living relatives of cetaceans, the artiodactyls^{8,9} (Fig. 2a). In contrast, *Remingtonocetus*, *Indocetus* and *Dorudon* all have small canal sizes that fall at the upper margin of the range of extant cetaceans (Fig. 2a). The size of the cochlea in extant and fossil cetaceans is close to that in other mammals (Fig. 2b), which confirms that the unprecedented size reduction specifically concerns the semicircular canals rather than the entire cetacean inner ear.

Functionally, the small semicircular canal size of cetaceans has been interpreted as a vestigial condition, in which receptors are lost because of limited neck and eye motility^{14,20}. However, the observed pattern of allometric scaling in parallel with terrestrial mammals points at structured functional adjustment of the system rather than degeneration and redundancy. Central to understanding the reduced canal size is that extant cetaceans, freed from the restrictions of gravitational pull and the need for substrate contact, are particularly acrobatic when compared with terrestrial animals of similar body size. Paradoxically, among non-cetacean mammals acrobatic species show canals with a relatively large arc^{14,15} (Fig. 1a). This increases the canals' sensitivity^{12,13}, and thus the ability to resolve small changes in angular head motion¹⁵. For animals showing fast and highly manoeuvrable locomotion such accurate sensory information is vital to maintain body coordination. Importantly, the canals of such species can be sensitive, without the risk of constant overstimulation, because they are part of a feedback system. The canals supply the vestibulo-collic reflex, which stabilizes the head by compensatory neck movements, thus keeping the input signal of the canals within limits. In extant cetaceans, however, reflex stabilization of the head is ineffective, because their streamlined bodies, marked by shortened and frequently fused cervical vertebrae, allow very little neck motility. The most plausible reason

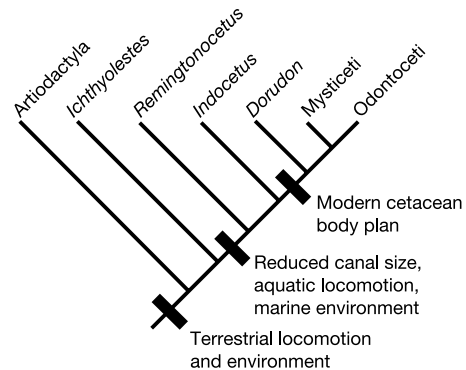


Figure 3 Cladogram showing the phylogenetic relationship of Eocene cetacean taxa examined here, their sister group the artiodactyls and the modern mysticetes and odontocetes. Key states of morphology, locomotion and environment are indicated. Modern cetacean bodyplan refers to, among other things, the total loss of hindlimb locomotor function and the presence of a tail fluke.

for the small arc size of their semicircular canals is thus to reduce sensitivity to match the high levels of uncompensated angular motion. In an aquatic environment this reduction is arguably less critical than in, for example, an arboreal setting where less accurate sensory clues easily impair locomotor control. The canal sizes of amphibious and aquatic, non-cetacean mammals in our sample are within the range for terrestrial species (Fig. 2a). However, none of these combine great aquatic agility with lack of neck motility.

The first appearance of small semicircular canals in the middle Eocene genera *Remingtonocetus* and *Indocetus* shows that the reduction in canal size took place rapidly and early in cetacean evolution, within five million years of the origin of the order. The palaeoenvironmental context of the fossils²⁴ demonstrates that this event accompanied the invasion of marine environments (Fig. 3). The newly evolved and highly derived vestibular sensory regime was almost certainly incompatible with any terrestrial locomotion beyond cautious beach-bound crawling, which indicates that dedicated agile swimming of cetaceans originated as a rapid and fundamental shift in behaviour. As such, the modification of the semicircular canal system represented a crucial 'point of no return' event in early cetacean evolution, which excluded a prolonged semi-aquatic phase. These findings strongly contrast with the pattern of gradual change shown by the postcranial skeleton, with the near-modern body plan and fluke-based propulsion of dorudontids emerging eight million years after the canal system modified (Fig. 3). In that period the well-developed hindlimbs of remingtonocetids and protocetids^{5,7,8} had a newly acquired function in powerful swimming, with some evidence pointing at a persisting degree of weight-bearing²⁵.

There remains the question of why *Remingtonocetus* and *Indocetus* would have shown increased levels of angular head motion, as is suggested by their reduced semicircular canal size. Although their neck length was shortened compared with pakicetids and other cursorial species^{9,26,27}, this was not to the extent seen in extant cetaceans. We hypothesize that the key underlying factor is the large, remarkably long-snouted head of Eocene cetaceans^{5,7,8}, including the oldest, terrestrial pakicetids⁹. When adapting to agile aquatic locomotion this particular morphology favours hydrodynamic integration of the head and trunk to reduce drag, minimizing neck movements at the cost of effective reflex stabilization of the head. The semicircular canals, as a functionally constrained sensory system, instantaneously adjusted to such a kinematic change, whereas skeletal modification leading to extreme shortening of the neck was a more gradual process.

Cetaceans are unusual in many ways, but well-known characters such as a relatively large brain, a tail fluke, echolocation, filterfeeding and mandibular hearing are all found in other mammals as well. The highly derived vestibular apparatus of cetaceans, on the other hand, is unique, and it is the first cetacean organ known to reach modern morphology. That early aquatic cetaceans had semicircular canals that do not resemble those of extant amphibious or aquatic non-cetacean mammals confirms that they behaved in ways that have no direct parallels among extant species. □

Methods

Size measurements of the semicircular canals and the cochlea were taken from computed tomography (CT) scans, plexiglas casts of the bony labyrinth, and the literature (Supplementary Information). CT scans, made with Siemens Somatom scanners at the National Museum of Natural History in Washington DC and the Hammersmith Hospital in London (*Dorudon atrox* only), have a pixel size of 0.1 mm, a slice thickness of 1.0 mm and a slice increment of 0.5 mm. CT scans of the other fossils and *Tursiops* were made with a Norland XCT Research M scanner, and these values are 0.07 mm, 0.50 mm and 0.25 mm, respectively. Scans were made coronally, and measurements were taken from planar reformatted images showing the full extent of each canal, using Voxblast 3.1 (Vaytek). Measurements of the casts were made using a binocular microscope. The literature sources used either give the required dimensions, list measurements from which they can be calculated, or include well-scaled images from which measurements can be taken.

The arc size of the semicircular canals was quantified by the radius of curvature, defined as half the average of the arc height and width (Fig. 1a; ref. 28). The results are

similar for the anterior, posterior and lateral canals so the mean of their three radii of curvature was used. The overall size of the cochlea was quantified by the mean of the 'slant height' and the diameters of the first and second turn. The slant height is the distance from the apex to the superiormost edge of the round window¹⁷, and the diameters were measured inferosuperiorly or mediolaterally, depending on the orientation of the cochlea. Owing to the preservation of the fossils the cochlear measurements could only be taken for *Ichthyolestes* and *Indocetus*.

Body mass data, including the estimates for the fossil taxa, are listed in the Supplementary Information. The estimate for *Remingtonocetus* is based on the mean value reported for *Dalanistes*⁵, which is closely related, but is 20% larger, and the estimate for *Indocetus* is the value reported for closely related and similar-sized *Rodhocetus*. The values are based on vertebral centrum size²⁷. The body mass of *Dorudon* is estimated from the full skeletal length of two adult specimens²⁹. The estimate for *Ichthyolestes* is based on bones of several individuals⁹. A braincase (H-GSP 98134) is identical in bizygomatic width (98 mm) to an average individual of *Canis latrans*. Long bones of *Ichthyolestes* (humerus, H-GSP 30128; femur, H-GSP 30420; tibia, H-GSP 98189) are similar in length to those of *Vulpes vulpes*, but are more robust. The body mass value of *Ichthyolestes* is taken as the mean of these two canids. Even considerable changes to these estimates do not alter the conclusions of the analyses.

Grade shifts in comparative studies can be demonstrated by inspecting the phylogenetically independent contrast of the basal node. Here, this is unnecessary because the grade shift in arc size shown by the non-pakicetid cetacean semicircular canals is unambiguous, marked by complete separation from the artiodactyls and other mammals (Fig. 2a). Three-dimensional reconstructions of the labyrinths in Fig. 1 were made with Voxell-man (Univ. of Hamburg)³⁰.

Received 25 July 2001; accepted 30 January 2002.

1. Thewissen, J. G. M. in *The Emergence of Whales* (ed. Thewissen, J. G. M.) 451–464 (Plenum, New York, 1998).
2. Schwartz, D. W. F. & Tomlinson, R. D. in *Neurotology* (eds Jackler, R. K. & Brackmann, D. E.) 59–98 (Mosby, St Louis, 1994).
3. Gingerich, P. D., Smith, B. H. & Simons, E. L. Hind limbs of Eocene *Basilosaurus*: evidence of feet in whales. *Science* **249**, 154–157 (1990).
4. Thewissen, J. G. M., Hussain, S. T. & Arif, M. Fossil evidence for the origin of aquatic locomotion in archaeocete whales. *Science* **263**, 210–212 (1994).
5. Gingerich, P. D., Arif, M., Clyde, W. C. New archaeocetes (Mammalia, Cetacea) from the middle Eocene Domanda Formation of the Sulaiman Range, Punjab (Pakistan). *Contrib. Mus. Paleontol. Univ. Michigan* **29**, 291–330 (1995).
6. Hulbert, R. C. in *The Emergence of Whales* (ed. Thewissen, J. G. M.) 235–267 (Plenum, New York, 1998).
7. Bajpai, S. & Thewissen, J. G. M. A new, diminutive Eocene whale from Kachchh (Gujarat, India) and its implications for locomotor evolution of cetaceans. *Curr. Sci.* **79**, 1478–1482 (2000).
8. Gingerich, P. D., Ul Haq, M., Zalmout, L. S., Khan, I. H. & Malkani, M. S. Origin of whales for early artiodactyls: hand and feet of Eocene Protocetidae from Pakistan. *Science* **293**, 2239–2242 (2001).
9. Thewissen, J. G. M., Williams, E. M. & Hussain, S. T. Skeletons of terrestrial cetaceans and the relationship of whales to artiodactyls. *Nature* **413**, 277–281 (2001).
10. Uhen, M. in *The Emergence of Whales* (ed. Thewissen, J. G. M.) 29–61 (Plenum, New York, 1998).
11. Thewissen, J. G. M. & Fish, F. E. Locomotor evolution in the earliest cetaceans: functional model, modern analogues, and paleontological evidence. *Paleobiology* **23**, 482–490 (1997).
12. Oman, C. M., Marcus, E. N. & Curthoys, I. S. The influence of the semicircular canal morphology on endolymph flow dynamics. *Acta Otolaryngol.* **103**, 1–13 (1987).
13. Muller, M. Semicircular duct dimensions and sensitivity of the vertebrate vestibular system. *J. Theor. Biol.* **167**, 239–256 (1994).
14. Spoor, F. & Zonneveld, F. Comparative review of the human bony labyrinth. *Yb. Phys. Anthropol.* **41**, 211–251 (1998).
15. Spoor, F. The semicircular canal system and locomotor behaviour, with special reference to hominin evolution. *Courier Forschungsinstitut Senckenberg* (in the press).
16. Hyrtl, J. *Vergleichend-anatomische Untersuchungen Über das innere Gehörorgan des Menschen und der Säugethiere* (Ehrlich, Prague, 1845).
17. Gray, A. A. *The Labyrinth of Animals* Vol. 2 (Churchill, London, 1908).
18. Yamada, M. & Yoshizaki, F. Osseous labyrinth of Cetacea. *Sci. Rep. Whale Res. Inst. (Tokyo)* **14**, 291–304 (1959).
19. Fleischer, G. Hearing in extinct cetaceans as determined by cochlear structure. *J. Paleontol.* **50**, 133–152 (1976).
20. Ketten, D. R. in *Marine Mammals Sensory Systems* (ed. Thomas, J.) 53–57 (Plenum, New York, 1992).
21. Luo, Z. & Eastman, E. R. Petrosal and inner ear of a squalodontoid whale: implications for evolution of hearing in odontocetes. *J. Vert. Paleont.* **15**, 431–442 (1995).
22. Luo, Z. & Marsh, K. Petrosal (periotic) and inner ear of a Pliocene kogiine whale (*Kogiinae*, Odontoceti): implications on the relationships and hearing evolution of toothed whales. *J. Vert. Paleontol.* **16**, 328–348 (1996).
23. Geisler, J. H. & Luo, Z. The petrosal and inner ear of *Herpetocetus* sp. (Mammalia: Cetacea) and their implications for the phylogeny and hearing of archaic mysticetes. *J. Paleontol.* **70**, 1045–1066 (1996).
24. Williams, E. M. in *The Emergence of Whales* (ed. Thewissen, J. G. M.) 1–28 (Plenum, New York, 1998).
25. Madar, S. I. in *The Emergence of Whales* (ed. Thewissen, J. G. M.) 353–377 (Plenum, New York, 1998).
26. Buchholtz, E. A. in *The Emergence of Whales* (ed. Thewissen, J. G. M.) 325–351 (Plenum, New York, 1998).
27. Gingerich, P. D. in *The Emergence of Whales* (ed. Thewissen, J. G. M.) 423–449 (Plenum, New York, 1998).
28. Spoor, C. F. & Zonneveld, F. W. Morphometry of the primate bony labyrinth: a new method based on high-resolution computed tomography. *J. Anat.* **186**, 271–286 (1995).
29. Marino, L. et al. Endocranial volume of mid-late Eocene archaeocetes (order: Cetacea) revealed by computed tomography: implications for cetacean brain evolution. *J. Mamm. Evol.* **7**, 81–94 (2000).
30. Höhne, K. H. et al. A new representation of knowledge concerning human anatomy and function. *Nature Med.* **1**, 506–511 (1995).

Supplementary Information accompanies the paper on *Nature's* website (<http://www.nature.com>).

Acknowledgements

We thank E. Allen, H. Chatterjee, J. Hooker, J. Mead, C. Potter and T. Yamada for access to specimens, and R. Barton, E. Blum, M. Colbert, C. Dean, J. DePonte, B. Frohlich, K. Grecco, K. H. Höhne, N. Jeffery, B. Jonsdottir, W. Jungers, R. Ketcham, K. Kupczik, D. Lieberman, Z. Luo, J. Moore, M. Muller, J. Neiger, C. Pellow, D. Plummer, A. Pommert, C. Ross, G. B. Schneider and A. Walker for their help. This research was supported by grants for the UCL Graduate School to F.S. and from the NSF to J.G.M.T. and S.T.H.

Competing interests statement

The authors declare that they have no competing financial interests.

Correspondence and requests for materials should be addressed to F.S. (e-mail: f.spoor@ucl.ac.uk).

Allometric cascade as a unifying principle of body mass effects on metabolism

Charles-A. Darveau*, Raul K. Suarez†, Russel D. Andrews* & Peter W. Hochachka*

* Department of Zoology, University of British Columbia, Vancouver, BC, V6T 1Z4, Canada

† Department of Ecology, Evolution, and Marine Biology, University of California, Santa Barbara, California 93106-9610, USA

The power function of basal metabolic rate scaling is expressed as aM^b , where a corresponds to a scaling constant (intercept), M is body mass, and b is the scaling exponent. The 3/4 power law (the best-fit b value for mammals) was developed from Kleiber's original analysis¹ and, since then, most workers have searched for a single cause to explain the observed allometry. Here we present a multiple-causes model of allometry, where the exponent b is the sum of the influences of multiple contributors to metabolism and control. The relative strength of each contributor, with its own characteristic exponent value, is determined by the control contribution. To illustrate its use, we apply this model to maximum versus basal metabolic rates to explain the differing scaling behaviour of these two biological states in mammals. The main difference in scaling is that, for the basal metabolic rate, the O₂ delivery steps contribute almost nothing to the global b scaling exponent, whereas for the maximum metabolic rate, the O₂ delivery steps significantly increase the global b value.

Until now, the classical approach to the basal metabolic rate (BMR) allometry problem has been to search for the single driving force or single rate-limiting step enforcing its scaling behaviour on overall metabolism. However, this concept in metabolic regulation studies was abandoned during the 1960s and was replaced by the concept of multiple control sites in metabolic pathways. By the 1980s and 1990s, rigorous mathematical models allowed control analysis to quantify the control contributions of different steps in metabolic pathways^{2–5} or in whole-organism physiological processes⁶. A key point, that control is vested in both energy supply and energy demand pathways^{3–5}, is important because many biologists estimate metabolic rate from O₂ uptake rates per gram per minute or from heat output rates. These parameter estimates are valid because they in turn are stoichiometrically related to complex pathways of adenosine triphosphate (ATP) synthesis rates and ATP utilization rates (however, see the discussion below on the 'O₂

wasting effect' of proton leak). In organisms at steady state the fluxes through ATP synthesis and utilization pathways are equal and mass-specific metabolic rate is equivalent to μmol s ATP cycled through ATP supply and ATP demand pathways per gram per minute. That is why it should not be surprising that modern metabolic studies identify regulatory roles in overall metabolic fluxes in both energy-supply and energy-demand pathways^{2–6}. In the traditional power function

$$\text{BMR} = aM^b \quad (1)$$

(a , M and b defined above), examination of the effects of body mass on metabolism should ideally consider the value of exponent b in equation (1) and the control contribution (or control coefficient) for each and every major step in ATP supply and ATP demand pathways in the system under investigation.

To sort out the varied contributions to control of net metabolic flux, say net O₂ flux, experimenters determine the fractional change in organismal O₂ flux caused by a fractional change in flux capacity through any given step or process in the path of O₂ from lungs to mitochondria in working tissues. The fractional change in organismal flux divided by the fractional change in capacity represents the control coefficient at each step^{2–6}. To illustrate, if the O₂ flux capacity of the lung is increased by 50% but only a 25% change in overall O₂ flux is achieved, the control coefficient for lung diffusion is 0.5, equal to the fractional change in overall O₂ flux divided by the fractional change in lung flux capacity. All the control coefficients in the pathway by definition add up to 1. In a system with a classical single rate-limiting step, say O₂ delivery^{7,8}, the control coefficient for that step would be essentially 1; that is, all control is vested in this process. The latter situation is never found in metabolic systems of any complexity^{3–6}. Under resting conditions all steps in the mammalian O₂ delivery chain necessarily display huge excess capacities and thus could not possibly be 'rate limiting' in the classical sense, while as we shall discuss further below, under maximum O₂ flux conditions, control is shared rather evenly among several major links in the chain. Hence the usually explicit, sometimes implicit, assumption of traditional allometry studies^{7,8}, that there is a single rate-limiting step or process that accounts for the b value in equation (1), is flawed.

We present here a multiple-causes model of allometry, in which there are multiple contributors to control, each with their own characteristic b values, that with their control contributions determine the value of the b scaling coefficient for overall energy metabolism. We can express this relationship as:

$$\text{MR} = a \sum c_i M^{b_i} \quad (2)$$

where MR is the metabolic rate in any given state, M is body mass, a is the intercept, b_i the scaling exponent of the process i , and c_i the control coefficient of the process i . (In most cases, a will be taken simply as the intercept, which is traditional in the allometry field. As ATP-utilizing processes are linked in parallel, each may have a unique a_i value; in sum these equal the baseline ATP turnover. On the energy supply side, the processes are linked in series with only one intercept at steady state indicating the same rate of baseline ATP turnover. For some purposes it is useful to decompose a into $a_{i,\text{max}}$ the flux capacity through step i , and f_i the fraction of $a_{i,\text{max}}$ used in a given metabolic state (see discussion below)).

Depending on metabolic state, the overall MR corresponds to the sum of the various contributors to ATP turnover, and the b exponent is the sum of the scaling exponents of all contributors, modulated by their control coefficients. In other words, each step in the linked series (that makes up the process, say O₂ flux, under study) possesses its own scaling behaviour, and its control coefficient c_i determines the degree to which its unique b_i exponent influences the global b value. For energy metabolism in mammals operating at varying rates between basal and maximum levels,